DTU Library

Broadband one-way propagation and rainbow trapping of terahertz radiations

Xu, Jie; Xiao, Sanshui ; Wu, Chiaho; Zhang, Hang; Deng, Xiaohua; Shen, Linfang

Link back to DTU Orbit

Broadband one-way propagation and rainbow trapping of terahertz radiations

Jie Xu,[1,2,3] **Sanshui Xiao,**[3] **Chiaho Wu,**[4] **Hang Zhang,**[4,5]
Xiaohua Deng,[2] **and Linfang Shen**[2,4,*]

[1]*College of Material Science and Engineering, Nanchang University, Nanchang 330031, China*
[2]*Institute of Space Science and Technology, Nanchang University, Nanchang 330031, China*
[3]*Department of Photonics Engineering, Technical University of Denmark, DK-2800 Kgs. Lyngby, Denmark*
[4]*Department of Applied Physics, Zhejiang University of Technology, Hangzhou 310023, China*
[5]*physzhang@zjut.edu.cn*
[*]*lfshen@zjut.edu.cn*

Abstract: Surface magnetoplasmon (SMP) supported at an interface between magnetized plasmonic and dielectric materials has been widely explored; however, it suffers with narrow bandwidth for one-way propagation. Here we propose a novel metal-semiconductor-dielectric-metal (MSDM) structure showing the large bandwidth for the complete one-way propagation (COWP). Because of the compression of the zone for two-way propagating modes in the semiconductor layer by reducing semiconductor thickness, the bandwidth is significantly increased by several times. More importantly, in such MSDM structure, the SMP dispersion can be engineered by controlling the semiconductor thickness, and based on this, slowing wave and trapping rainbow can be realized in a tapered system at terahertz frequencies.

1. Introduction

One-way propagating electromagnetic (EM) modes, which are similar to the chiral edge states found in the quantum-Hall effect [1], have received strong interest recently [2–5]. One-way EM modes are such modes that are allowed to propagate in only one direction, and because of the absence of backpropagating mode in the waveguide system, they are immune to backscattering at imperfections or bends. One-way modes provide a basic mechanism for realizing new classes of photonic devices that would be impossible using conventional reciprocal modes [6]. It was reported that one-way EM modes can be sustained by the edges of two-dimensional photonic crystals made of magnetic-optical (MO) materials, where time-reversal symmetry is broken by applying dc magnetic field [7–10]. The existence of such modes has been experimentally verified by using (gyromagnetic) yttrium-iron-garnet (YIG) in the microwave regime [11]. One-way EM mode of different type, which is based on surface plasmons (SPs) [12], has also been proposed [13]. It seems to be more attractive owing to its robustness in mechanism and simpleness in configuration [14–16].

Surface plasmons (SPs) sustained by the interface of plasmonic material and dielectric become nonreciprocal under an external dc magnetic field [17, 18]. When the cyclotron frequency of electron (ω_c) in the plasmonic material is comparable with the plasma frequency, the SP asymptotic frequency differs remarkably in the forward and backward directions, making SP propagate unidirectionally within the interval between the two different asymptotic frequencies [13, 15]. SPs in magnetized plasmonic material is generally referred to as surface magnetoplasmons (SMPs) [17]. Generally a semiconductor possesses a plasma frequency in terahertz regime and the electron effective mass is far less than the electron mass, thus the electron cyclotron frequency is often comparable with the plasma frequency under normal magnetic field intensity. Therefore, one-way SMPs is realizable at terahertz frequencies by using semiconductors [14]. In a semiconductor-dielectric-metal (SDM) layered structure, it was shown that one-way SMPs can be

immune to backscattering, thus exhibiting the complete one-way propagation (COWP) [15, 19].

It is reported more recently that by using robust one-way SMPs, extraordinary cavities that breaks time-bandwidth limit in physics can be constructed [6]. However, in the previous SDM structure, the COWP bandwidth of SMPs is very limited, e.g., the maximal value is only $0.03\omega_p$ (where ω_p is the plasma frequency) in the case if the dielectric is air. In this paper, we will investigate theoretically SMPs in a metal-semiconductor-dielectric-metal (MSDM) layered structure. It will be shown that the semiconductor thickness in the MSDM structure can greatly affect the COWP band. Compared with the previous SDM structure, the dependence of the COWP bandwidth on ω_c is significantly improved, thus broadband SMPs become available in the MSDM structure. It will also be shown that in the MSDM structure, the COWP bandwidth can be largely increased by optimizing the semiconductor thickness. Moreover, interesting phenomenon based on the effect of the semiconductor thickness is numerically demonstrated.

Slowing EM waves is believed to be an attractive technique for enhanced nonlinear optics [20], light harvesting [21], and optical signal processing [22, 23]. Recently, the concept of a "trapped rainbow" has generated considerable interest for potential use in optical data storage and processing [23]. It aims to trap different frequency components of the wave packet at different positions in space permanently. More recently, it was reported that trapped rainbow can be realized by using SMPs [24]. In our proposed MSDM structure, it will be shown that the SMP dispersion can be engineered by controlling the semiconductor thickness. Based on that mechanism, slowing wave and trapping rainbow can be achieved in a tapered MSDM system. Different from Ref. 21, where a tapered external magnetic field is required, only the semiconductor thickness is tapered in our system for trapped rainbow, so our approach seems to be more feasible in practice. The phenomena of trapped rainbow in a tapered MSDM system will be numerically demonstrated.

2. Physical model

The physical model for sustaining broadband one-way SMPs at terahertz frequencies is illustrated in Fig. 1(a). This waveguide system is a metal-semiconductor-dielectric-metal (MSDM) layered structure, with an external dc magnetic field applied to break the time-reversal symmetry. The metal is assumed to be perfectly electric conductor, which is a good approximation for the terahertz regime. The dielectric layer with the relative permittivity ε_r has a thickness of d_1, and the semiconductor layer has a thickness of d_2. The external magnetic field introduces gyroelectric anisotropy in the semiconductor, thus its relative permittivity has the form [15, 17]

$$\overset{\leftrightarrow}{\varepsilon} = \begin{bmatrix} \varepsilon_1 & 0 & i\varepsilon_2 \\ 0 & \varepsilon_3 & 0 \\ -i\varepsilon_2 & 0 & \varepsilon_1 \end{bmatrix},$$ (1)

with $\varepsilon_1 = \varepsilon_\infty \left(1 - \frac{\omega_p^2}{\omega^2 - \omega_c^2} \right), \varepsilon_2 = \varepsilon_\infty \frac{\omega_c \omega_p^2}{\omega(\omega^2 - \omega_c^2)}, \varepsilon_3 = \varepsilon_\infty \left(1 - \frac{\omega_p^2}{\omega^2} \right)$, where ω is the angular frequency, ω_p is the plasma frequency, $\omega_c = eB_0/m^*$ (where e and m^* are, respectively, the charge and effective mass of a electron) is the electron cyclotron frequency, and ε_∞ is the high-frequency (relative) permittivity. Compared with the previous system for one-way SMPs, which is a semiconductor-dielectric-metal (SDM) layered structure as shown in Fig. 1(b), the semiconductor is terminated by a metal slab in the present system. Therefore, the EM modes in the semiconductor become bound modes in the present system, which must satisfy transverse resonance condition, and their modal properties should be closely dependent on the semiconductor thickness [25]. These bound modes are guided by means of zigzag reflections at the metal surface and semiconductor-dielectric interface, and they are usually allowed to propagate both forward and backward. We refer to these two-way (propagating) modes as normal modes in order to distinguish them with SMPs.
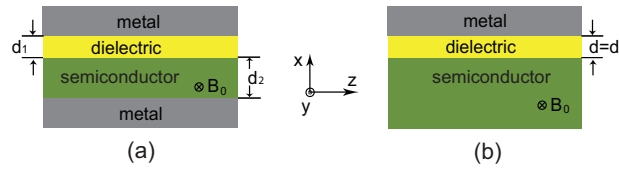
Fig. 1. Schematics of the metal-semiconductor-dielectric-metal (a) and related semiconductor-dielectric-metal (b) structures for sustaining one-way SMPs. An external dc magnetic field is applied along the $-y$ direction in the two structures.

We first investigate SMPs in the system under our consideration. The EM fields of SMPs are H-polarized, and the nonzero component of the magnetic field can be written as

$$H_y(x, z) = [A_1 \exp(-\alpha_d x) + A_2 \exp(\alpha_d x)] \exp(ikz) \tag{2}$$

in the dielectric layer for $0 < x \leq d_1$ and

$$H_y(x, z) = [B_1 \exp(\alpha_s x) + B_2 \exp(-\alpha_s x)] \exp(ikz) \tag{3}$$

in the semiconductor layer for $-d_2 \leq x < 0$, where k is the propagation constant, $\alpha_d = \sqrt{k^2 - \varepsilon_r k_0^2}$ (where k_0 is the wavenumber in vacuum), and $\alpha_s = \sqrt{k^2 - \varepsilon_v k_0^2}$ with $\varepsilon_v = \varepsilon_1 - \varepsilon_2^2/\varepsilon_1$ being the Voigt permittivity. The nonzero components (E_x and E_z) of the electric field can be obtained straightforwardly from H_y. The tangential component E_z must vanish at the metal boundaries $x = d_1$ and $-d_2$, yielding that $A_2 = A_1 \exp(-2\alpha_d d_1)$ and $B_2 = B_1[(\varepsilon_1 \alpha_s + \varepsilon_2 k)/(\varepsilon_1 \alpha_s - \varepsilon_2 k)] \exp(-2\alpha_s d_2)$. The boundary conditions further require the field components E_z and H_y to be continuous at the interface $x = 0$, and based on which we can obtain

$$\left(k^2 - \varepsilon_1 k_0^2\right) \tanh(\alpha_s d_2) + \frac{\varepsilon_1}{\varepsilon_r} \alpha_d \left[\alpha_s - \frac{\varepsilon_2}{\varepsilon_1} k \tanh(\alpha_s d_2)\right] \tanh(\alpha_d d_1) = 0, \tag{4}$$

which is the dispersion relation for SMPs. The linear term in Eq. (4) with respect to k indicates that SMPs are nonreciprocal in the system. From Eq. (4) we find

$$\omega_{sp}^{(1)} = \frac{1}{2} \left(\sqrt{\omega_c^2 + 4 \frac{\varepsilon_\infty}{\varepsilon_\infty + \varepsilon_r} \omega_p^2} + \omega_c \right). \tag{5}$$

for $k \to +\infty$, and

$$\omega_{sp}^{(2)} = \frac{1}{2} \left(\sqrt{\omega_c^2 + 4 \frac{\varepsilon_\infty}{\varepsilon_\infty + \varepsilon_r} \omega_p^2} - \omega_c \right), \tag{6}$$

$$\omega_{sp}^{(3)} = \omega_c, \tag{7}$$

for $k \to -\infty$. Evidently, $\omega_{sp}^{(1)}$ and $\omega_{sp}^{(2)}$ represent the two asymptotic frequencies of SMPs (in the opposite directions) which are supported by the interface of the semiconductor and dielectric, and they are identical to those in the previous SDM system [15]. The dispersion relation of SMPs in the SDM system reads

$$\alpha + \frac{\varepsilon_2}{\varepsilon_1} k + \frac{\varepsilon_v}{\varepsilon_r} \alpha_d \tanh(\alpha_d d) = 0, \tag{8}$$

which can be obtained from Eq. (4) by letting $d_2 \to \infty$. $\omega_{sp}^{(3)}$ in Eq. (7) corresponds to the asymptotic frequency of another SMP branch, which is supported by the interface of the
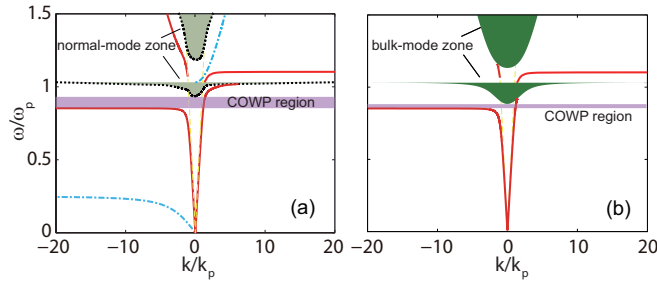
Fig. 2. Dispersion relations of SMPs in the MSDM (a) and SDM (b) systems. Solid and dot-dashed lines correspond to SMPs supported by the dielectric-semiconductor and metal-semiconductor interfaces, respectively. Dotted lines in (a) represent the dispersion curves for normal modes with lowest order in the semiconductor layer, and shaded areas in (b) represent bulk-mode zones for the semiconductor itself. The shaded rectangle in (a) and (b) represents the COWP region and dashed lines the light line in air. The parameters of the two systems are as follows: $\varepsilon_r = 1$, $d_1 = 0.1\lambda_p$; $\omega_c = 0.25\omega_p$, $d_2 = 0.2\lambda_p$.

semiconductor and metal in the MSDM system. In this paper, the semiconductor is assumed to be InSb with $\epsilon_\infty = 15.6$ and $\omega_p = 4\pi \times 10^{12}$ rad/s [26]. The dielectric layer is air with $\varepsilon_r = 1$, and its thickness is set to be $d_1 = 0.1\lambda_p$ (where $\lambda_p = 2\pi c/\omega_p$ with c being the light speed in vacuum), for which it can sustain no mode which is guided by a means of zigzag reflections at the surfaces of the metal and semiconductor [15].

Figure 2(a) shows the dispersion relation of SMPs in the MSDM system. As an example, the parameters are taken as follows: $d_2 = 0.2\lambda_p$ and $\omega_c = 0.25\omega_p$ (i.e., $B_0 = 0.25$T). For comparison, the dispersion relation of SMPs in the corresponding SDM system is plotted in Fig. 2(b). Obviously, for SMPs supported by the semiconductor-dielectric interface (solid lines), the dispersion curves are similar for $k < 0$ in the two systems, but they are rather different for $k > 0$ because of difference between the normal-mode and bulk-mode zones. Note that the dispersion branch of SMPs with $k > 0$ are actually cut into two segments by the normal-mode zone or bulk-mode zone. In the SDM system, bulk modes in the semiconductor are space waves, which are described by $\sqrt{k_x^2 + k_z^2} = \sqrt{\varepsilon_v}k_0$. The bulk-mode zones in the SDM system are represented by the shaded areas in Fig. 2(b), and there are two zones where $\varepsilon_v > 0$. The lower bulk-mode zone has a low-frequency cutoff given by

$$\omega_{cf,b} = \frac{1}{2}\left(\sqrt{\omega_c^2 + 4\omega_p^2} - \omega_c\right), \tag{9}$$

which determines the upper limit of the COWP region. For $\omega_c = 0.25\omega_p$, we find that $\omega_{cf,b} = 0.8828\omega_p$. In the present MSDM system, normal modes guided by the semiconductor layer are somewhat similar to bulk modes, whose transverse components (k_x) of wavevectors are real-valued in the semiconductor, and the dispersion relation for them can be derived from Eq. (4) by letting $k = k_z$ and $\alpha_s = ik_x$ (where k_x and k_z are both real-valued), and it has the form

$$\left(k_z^2 - \varepsilon_1 k_0^2\right)\tan(k_x d_2) + \frac{\varepsilon_1}{\varepsilon_r}\alpha_d\left[k_x - \frac{\varepsilon_2}{\varepsilon_1}k_z \tan(k_x d_2)\right]\tanh(\alpha_d d_1) = 0, \tag{10}$$

where $\alpha_d = \sqrt{k_z^2 - \varepsilon_r k_0^2}$ (which is allowed to be real or imaginary number). Note that k_x and k_z must also satisfy the dispersion relation for the semiconductor, i.e., $\sqrt{k_x^2 + k_z^2} = \sqrt{\varepsilon_v}k_0$. Therefore, for a given ω, there exist only discrete solutions for k_z or k_x, which correspond to the transverse
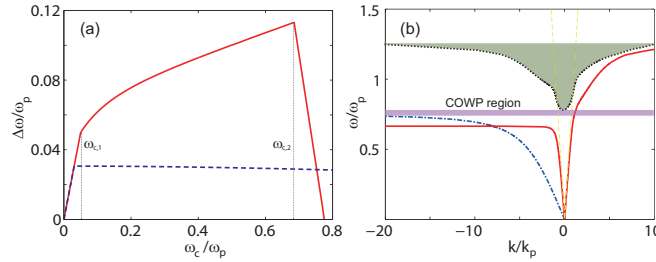
Fig. 3.   (a) COWP bandwidth ($\Delta\omega_{cowp}$) as a function of ω_c in the MSDM system. The corresponding COWP bandwidth (dashed line) for the SDM system is included for comparison. (b) Dispersion relation of SMPs in the MSDM system when $\omega_c = 0.75\omega_p$. Solid and dot-dashed lines correspond to SMPs supported by the dielectric-semiconductor and metal-semiconductor interfaces, respectively. Dotted line represents the dispersion curve for the normal mode with lowest order in the semiconductor layer, and shaded rectangle represents the COWP region. The other parameters are the same as in Fig. 2.

resonances of different orders in the MSDM system. With Eq. (10), the normal mode with the lowest order, which possesses the lowest cutoff, is calculated and plotted in Fig. 2(a) as dotted line. For consistency, this cutoff is also denoted by $\omega_{cf,b}$, and it is found to be $\omega_{cf,b} = 0.933\omega_p$, which is obviously larger than the value for the SDM system.

3.   COWP bandwidth of SMPs

As in the SDM system, there exists a frequency range in the MSDM system, where SMPs with $k > 0$ exhibit complete one-way propagation (COWP). The COWP band must lie within the band gap of bulk or normal modes in the semiconductor. In both Figs. 2(a) and 2(b), the COWP band ranges from $\omega_{sp}^{(2)}$ to $\omega_{cf,b}$, and its bandwidth is $\Delta\omega_{cowp} = \omega_{cf,b} - \omega_{sp}^{(2)}$. The COWP region is indicated by the shaded rectangle. We find that $\Delta\omega_{cowp} = 0.0806\omega_p$ in Fig. 2(a) and $\Delta\omega_{cowp} = 0.0304\omega_p$ in Fig. 2(b). The COWP bandwidth in the MSDM system is 2.65 times larger than that in the SDM system. But note that $\Delta\omega_{cowp} = \omega_c$ for both the systems if $\omega_{sp}^{(1)} \leq \omega_{cf,b}$. Both $\omega_{sp}^{(1)}$ and $\omega_{cf,b}$ are closely dependent on ω_c, and we denote the critical ω_c value by $\omega_{c,1}$, at which $\omega_{sp}^{(1)} = \omega_{cf,b}$. For the SDM system, it is found that

$$\omega_{c,1} = \frac{\varepsilon_r}{\sqrt{2\left(\varepsilon_r + 2\varepsilon_\infty\right)\left(\varepsilon_r + \varepsilon_\infty\right)}}\omega_p, \tag{11}$$

and it has $\omega_{c,1} = 0.0306\omega_p$ ($B_0 = 0.0306$T) for $\varepsilon_r = 1$. For the MSDM system, however, our numerical calculation shows that $\omega_{c,1} = 0.04956\omega_p$ ($B_0 = 0.04956$T) when $d_2 = 0.2\lambda_p$. Figure 3(a) shows the dependence of $\Delta\omega_{cowp}$ on ω_c for the both systems, where the parameters are the same as in Fig. 2 (except for ω_c). For the MSDM system, $\Delta\omega_{cowp} = \omega_c$ when $\omega_c \leq \omega_{c,1}$, where $\omega_{c,1} = 0.04956\omega_p$, and interestingly, $\Delta\omega_{cowp}$ grows with ω_c even when $\omega_c > \omega_{c,1}$, which is quite different from the situation for the SDM system. For the SDM system, $\Delta\omega_{cowp}$ decreases with ω_c when $\omega_c > \omega_{c,1}$, and it has a maximum of $0.0306\omega_p$ at $\omega_c = \omega_{c,1}$, where $\omega_{c,1} = 0.0306\omega_p$.

   For the MSDM system with $d_2 = 0.2\lambda_p$, when ω_c grows from $\omega_{c,1}$ to $0.5\omega_p$ ($B_0 = 0.5$T), $\Delta\omega_{cowp}$ increases from $0.04956\omega_p$ to $0.1\omega_p$, as seen in Fig. 3(a). So large COWP bandwidth can be achieved for the MSDM system by increasing external magnetic field. However, as seen in Fig. 3(a), when ω_c further increases and is larger than a certain value, which we denote by

$\omega_{c,2}$, $\Delta\omega_{cowp}$ begins to quickly decrease with ω_c. This critical value for ω_c is found to be

$$\omega_{c,2} = \sqrt{\frac{\varepsilon_\infty}{2(\varepsilon_\infty + \varepsilon_r)}}\omega_p, \tag{12}$$

at which $\omega_{sp}^{(2)} = \omega_{sp}^{(3)}$. We find that $\omega_{c,2} = 0.6855\omega_p$ for $\varepsilon_r = 1$. Note that for the MSDM system $\omega_{c,1}$ depends on d_2 but $\omega_{c,2}$ does not. In the case when $\omega_c > 0.6855\omega_p$, $\omega_{sp}^{(3)} > \omega_{sp}^{(2)}$, thus the lower COWP limit is determined by $\omega_{sp}^{(3)}$ instead of $\omega_{sp}^{(2)}$. To show this, the dispersion diagram for the MSDM system with $\omega_c = 0.75\omega_p$ ($B_0 = 0.75$T) is displayed in Fig. 3(b).

As the cutoff frequency $\omega_{cf,b}$ shifts up in the MSDM system when d_2 decreases, it is naturally desired that the COWP bandwidth can be effectively increased by reducing d_2. To clarify this, the MSDM systems with different d_2 values are analyzed. The other parameters of the MSDM systems are kept to be $\omega_c = 0.5\omega_p$ ($B_0 = 0.5$T), $d_1 = 0.1\lambda_p$, and $\varepsilon_r = 1$. Figures 4(a)-4(d) show the dispersion diagrams for the cases of $d_2 = 0.2\lambda_p$, $0.1\lambda_p$, $0.05\lambda_p$, and $0.03\lambda_p$, respectively. Obviously, the cutoff of the lowest-order normal mode, which determines the upper COWP limit (ω_u), shifts up when d_2 is reduced. We find that $\omega_{cf,b} = 0.7511\lambda_p$ for $d_2 = 0.2\lambda_p$, $\omega_{cf,b} = 0.7669\lambda_p$ for $d_2 = 0.1\lambda_p$, $\omega_{cf,b} = 0.8824\lambda_p$ for $d_2 = 0.05\lambda_p$, and $\omega_{cf,b} = 0.9864\lambda_p$ for $d_2 = 0.03\lambda_p$. However, in the later three cases, the SMP dispersion curve with $k < 0$ is out of shape, and a peak appears at a finite $|k|$ value. In this situation, the lower limit (ω_l) of the COWP band is determined by the top of that peak instead of ω_{sp}^-. The dependences of ω_u and ω_l on d_2 are shown in Fig. 5(a). ω_u decreases with d_2, and this is also the situation for ω_l in the case when $d_2 < 0.14\lambda_p$. But ω_l becomes a constant of $\omega_{sp}^{(2)}$ when $d_2 \geq 0.14\lambda_p$. In this case, the peak of the dispersion curve with $k < 0$ disappears, and its highest frequency is the asymptotic frequency $\omega_{sp}^{(2)}$, by which ω_l is determined. Figure 5(b) shows the COWP bandwidth ($\Delta\omega_{cowp} = \omega_u - \omega_l$) as a function of d_2. It is found that $\Delta\omega_{cowp}$ reaches a maximum of $0.1956\omega_p$ at $d_2 = 0.08\lambda_p$, which is 6.4 times larger than the maximal value for the SDM system.
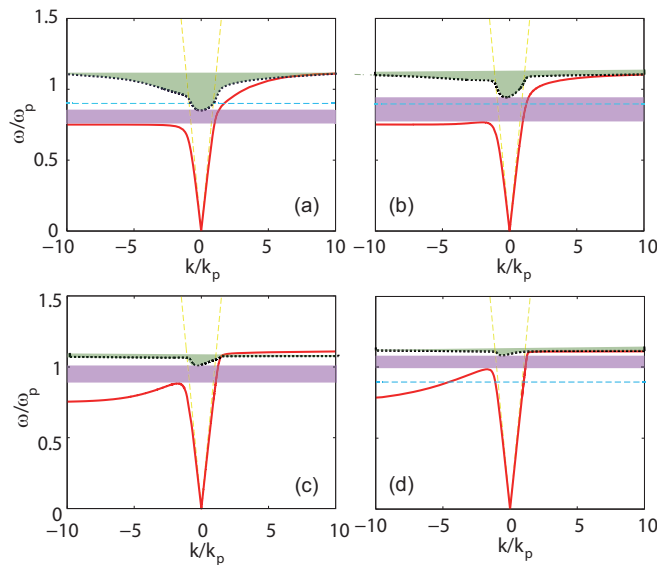

Fig. 4. Dispersion curves for SMPs (solid) and lowest-order normal mode (dotted) in the MSDM system for different d_2 values. (a) $d_2 = 0.2\lambda_p$, (b) $d_2 = 0.1\lambda_p$, (c) $d_2 = 0.05\lambda_p$, (d) $d_2 = 0.03\lambda_p$. The horizontal dashed line indicates the frequency $\omega = 0.9\omega_p$. $\omega_c = 0.5\omega_p$, and the other parameters are the same as in Fig. 2.
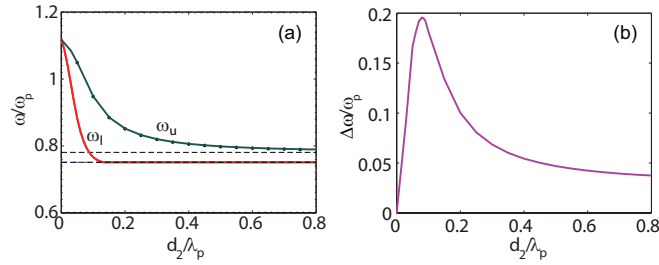
Fig. 5. (a) Upper (ω_u) and lower (ω_l) limit frequencies of the COWP band as functions of d_2. (b) COWP bandwidth as a function of d_2. $\omega_c = 0.5\omega_p$, and other parameter are the same as in Fig. 2.
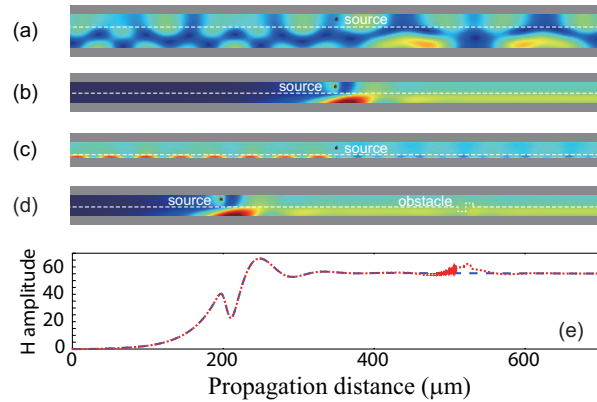

Fig. 6. (a)-(c) Simulated magnetic field amplitudes in the MSDM systems with different d_2 values. (a) $d_2 = 0.2\lambda_p$, (b) $d_2 = 0.1\lambda_p$, and (c) $d_2 = 0.03\lambda_p$. (d) Simulated magnetic field amplitudes in the MSDM system of $d_2 = 0.1\lambda_p$ but with an obstacle. The obstacle consists of two square columns of air and semiconductor, which are respectively located below and above the semiconductor surface. The white dashed line in (a)-(d) indicates the semiconductor surface. (e) Magnetic field amplitudes along a horizontal line at the semiconductor surface in (b) (dashed line) and (d) (dotted line). For each case, the source with the frequency $f = 1.8$ THz lies at $d_1/2$ above the semiconductor surface. The semiconductor is lossy with $\nu = 0.01\omega_p$. $\omega_c = 0.5\omega_p$, and the other parameters are the same as in Fig. 2.

From the above analysis, it is clear that the COWP band is greatly affected by the semiconductor thickness. To vividly illustrate this, by using the finite-element method (FEM), we performed the simulation of wave transmission in the MSDM system, and three cases were considered: $d_2 = 0.2\lambda_p$, $d_2 = 0.1\lambda_p$, and $d_2 = 0.03\lambda_p$. The other parameters are the same as in Fig. 4. In the simulation, a linear magnetic current, which lay at $d_1/2$ (i.e., 7.5 μm) above the semiconductor surface, was used to excite waves, and its frequency was set to be $f = 1.8$ THz, i.e., $\omega = 0.9\omega_p$. To obtain a steady-state solution in the frequency domain, the semiconductor loss was taken into account. For lossy semiconductor, the expressions for ε_1 and ε_2 in Eq. (1) become

$$\varepsilon_1 = \varepsilon_\infty \left\{ 1 - \frac{(\omega + i\nu)\omega_p^2}{\omega[(\omega + i\nu)^2 - \omega_c^2]} \right\}, r \tag{13}$$

$$\varepsilon_2 = \varepsilon_\infty \frac{\omega_c\omega_p^2}{\omega[(\omega + i\nu)^2 - \omega_c^2]}, \tag{14}$$

where ν is the electron scattering frequency. We took $\nu = 0.01\omega_p$ in the simulation. Figures

6(a)-6(c) show the simulated magnetic field amplitudes. Obviously, in the case of $d_2 = 0.2\lambda_p$, waves excited by the source are allowed to propagate in both the forward and backward directions [see Fig. 6(a)], and in the case when $d_2 = 0.1\lambda_p$, waves are only allowed to propagate forward [see Fig. 6(b)], exhibiting the one-way propagation behaviour. However, in the case when $d_2 = 0.03\lambda_p$, the situation [see Fig. 6(c)] seems to revert to the first case of $d_2 = 0.2\lambda_p$. These phenomena are in good agreement with the dispersion properties of the MSDM system in Fig. 4, where the frequency $\omega = 0.9\omega_p$ is indicated by a horizontal dashed line.

To verify the robustness of the one-way propagation in the MSDM system, we further introduced an obstacle into the MSDM system with $d_2 = 0.1\lambda_p$. The obstacle consists of a air and semiconductor columns, which are respectively located below and above the semiconductor surface at a distance of 320 μm from the source [see Fig. 6(d)]. Both columns have the same rectangular cross-section with length 10 μm and width 5 μm. The simulated results are plotted in Fig. 6(d). Evidently, when propagating-forward wave (excited by the source) reaches the obstacle, it goes around the obstacle. The backscattering of wave by the obstacle is completely suppressed, because there exists no backward-propagating mode in this MSDM system. Compared with Fig. 6(b), the field of SMPs in Fig. 6(d) is only modified locally around the obstacle. In Fig. 6(d), the fields in front of and behind the obstacle are almost identical. This is more clearly displayed in Fig. 6(e), where the magnetic field amplitudes along the semiconductor surface ($x = 0$) are plotted for the cases in Figs. 6(b) and 6(d).

Finally, we examine the influence of semiconductor loss on SMPs and make a related comparison between the MSDM and SDM systems. The parameters of the systems are taken as follows: $\omega_c = 0.5\omega_p$ ($B_0 = 0.5$ T), $d_1 = 0.1\lambda_p$, $d_2 = 0.2\lambda_p$ and $\nu = 0.01\omega_p$. In the lossy case, the propagation constant of SMPs becomes complex, i.e., $k = k_r + ik_i$ (where both k_r and k_i are real-valued), and it can be accurately solved from Eq. (4). The propagation length of SMPs can be defined by $L_p = 1/(2k_i)$. For the frequency $f = 1.52$ THz (i.e., $\omega = 0.76\omega_p$), we find that $L_p = 3024$ μm for the MSDM system and $L_p = 2403$ μm for the SDM system. Compared with the SDM system, the portion of the EM energy of SMPs in the semiconductor should be substantially reduced for the MSDM system, therefore SMPs has larger propagation length there.
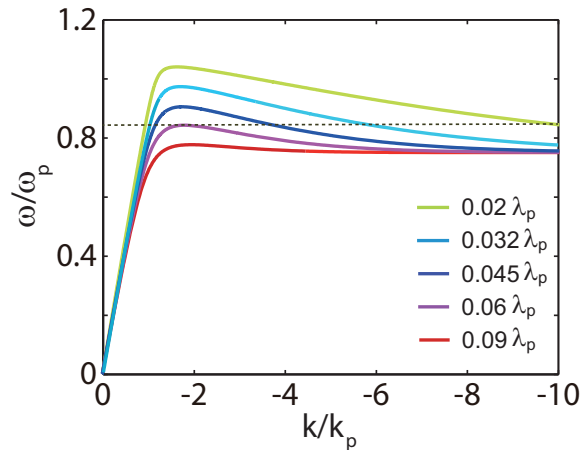
4. Trapped rainbow in a tapered system

Fig. 7. SMP bands (with the asymptotic frequency $\omega_{sp}^{(2)}$) for different d_2 values. From top to bottom: $d_2 = 0.02\lambda_p, 0.032\lambda_p, 0.045\lambda_p, 0.06\lambda_p$, and $0.09\lambda_p$. $\omega_c = -0.5\omega_p$, and the other parameters are the same as in Fig. 2.

It is interesting that one branch of SMPs with the asymptotic frequency $\omega_{sp}^{(2)}$ in the MSDM system is humped in the negative k region when the semiconductor layer is thin enough. This humped SMP band can be transferred to the positive k region by reversing the external magnetic field, as shown in Fig. 7, where $\omega_c = -0.5\omega_p$. In such humped band, the group velocity ($v_g = d\omega/dk$) vanishes at the top of the peak, i.e., at the highest frequency for SMPs propagating forward in the case of $\omega_c < 0$, and we denote this frequency by f_0. Obviously, f_0 is larger than $\omega_{sp}^{(2)}$ described in Eq. (6). Furthermore, f_0 is a function of d_2, i.e., $f_0 = f_0(d_2)$, and it decreases when d_2 increases, as illustrated in Fig. 7, where the cases with various d_2 values are displayed. Suppose that f_0 decreases with the propagation distance in a tapered MSDM structure, where the semiconductor thickness is linearly increased along the propagation direction. In such tapered structure, an incident wave with a certain frequency f would be slowed down as it propagates
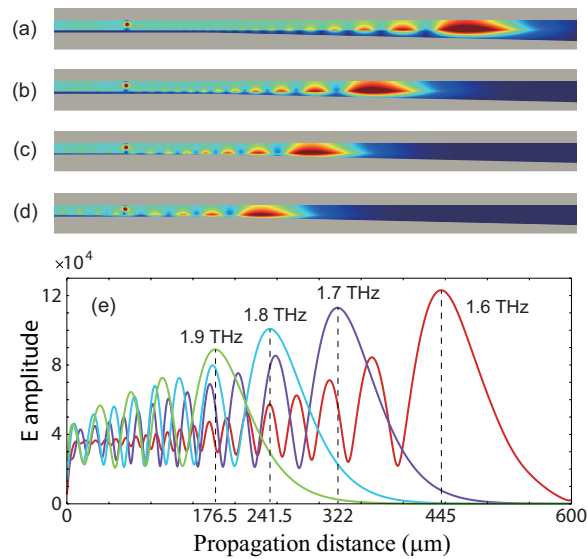

Fig. 8. (a)-(d) Simulated electric field amplitudes for different frequencies in a system consisting of a uniform and tapered MSDM structures. (a) 1.6 THz, (b) 1.7 THz, (c) 1.8 THz, and (d) 1.9 THz. In the system, the semiconductor thickness is $d_2 = 0.03\lambda_p$ in the uniform section of the length 200 μm, and in the tapered section, it linearly increases from $0.03\lambda_p$ to $0.09\lambda_p$ over the length 500 μm. (e) Electric field amplitudes along the semiconductor surface in (a)-(d). The source lies at $d_1/2$ above the semiconductor surface in the uniform section. $\omega_c = -0.5\omega_p$, $\nu = 0.01\omega_p$, and the other parameters are the same as in Fig. 2.

forward. When it reaches a critical point, at which f_0 is equal to f, it would be stopped because its group velocity vanishes there. Behind the critical position, $f_0 < f$, so the wave is prohibited to propagate forward. Evidently, waves with different frequencies would be stopped at different positions along the propagation direction, and a phenomenon similar to the "trapped rainbow" would occur [23].

To verify the phenomenon of trapped rainbow, we performed the simulation of wave transmission in a properly designed system with the FEM. The system consists of two sections, one is a uniform MSDM structure with $d_2 = 0.03\lambda_p$ and the length 200 μm, the other is a tapered MSDM structure, where d_2 is linearly increased from $0.03\lambda_p$ to $0.09\lambda_p$ over its length 500 μm. In the simulation, we took $\omega_c = -0.5\omega_p$, and other parameters of the system were the same as in Fig. 6. The source (i.e., linear magnetic current) was placed at $d_1/2$ above the semiconductor surface in the uniform section, and four different frequencies were considered: $f = 1.6$ THz, 1.7 THz, 1.8 THz, and 1.9 THz. The simulated electric-field amplitudes for the four frequencies are

plotted in Figs. 8(a)-8(d), respectively. As expected, waves at the four frequencies are all stopped in the tapered section, and the one with lower frequency is stopped at a larger distance from the source. At the position where a wave stops, a hotspot with significantly enhanced electric field is generated for each case. Figure 8(e) shows the electric field amplitudes along the semiconductor surface for the four cases. Obviously, the electric field is only increased by several times at the hotspot, compared with the fields in the uniform section. We think that the field enhancement is so limited because the hotspot has a large longitudinal size, as shown in Fig. 8. The hotspot occurring at larger d_2 has a larger field enhancement, which means that the related SMPs have a smaller modal size (in the transverse direction), and this agrees well with larger propagation constant at the peak of the corresponding dispersion band, as shown in Fig. 7.

5. Conclusion

In conclusion, we have systemically studied dispersion properties of SMPs and normal modes in the MSDM structure. It has been shown that the lower cutoff of normal modes in the semiconductor layer shifts up when the semiconductor thickness reduces, thus the COWP band for SMPs can be largely broaden. Compared with the SDM structure, the COWP bandwidth of SMPs possesses essentially different relation with the external magnetic field in the MSDM structure, thus the previous limit to its growth is removed. For the example of the dielectric being air, the COWP bandwidth in the MSDM structure can be six times larger than the maximal value in the previous SDM structure. More importantly, it has been shown that the dispersion of SMPs in the MSDM structure can be engineered by controlling the semiconductor thickness, and the group velocity of SMPs may vanishes at a certain frequency and finite propagation constant. Based on that mechanism, "trapped rainbow" has been numerically demonstrated at terahertz frequencies in a MSDM system where the semiconductor thickness is tapered along the propagation distance.

Funding

Disclosures

The authors declare that there are no conflicts of interest related to this article.

References

1. R. E. Prange and S. M. Girvin, *The Quantum Hall Effect* (Springer, 1987).
2. F. D. M. Haldane and S. Raghu, "Possible realization of directional optical waveguides in photonic crystals with broken time-reversal symmetry," Phys. Rev. Lett. **100**(1), 013904 (2008).
3. S. A. Skirlo, L. Lu, and M. Soljačić, "Multimode one-way waveguides of large Chern numbers," Phys. Rev. Lett. **113**(11), 113904 (2014).
4. L. Lu, J. D. Joannopoulos, and M. Soljačić, "Topological photonics," Nat. Photonics **8**(11), 821-829 (2014).
5. A. B. Khanikaev and G. Shvets, "Two-dimensional topological photonics," Nat. Photonics **11**(12), 763-773 (2017).
6. K. L. Tsakmakidis, L. Shen, S. A. Schulz, X. Zheng, J. Upham, X. Deng, H. Altug, A. F. Vakakis and R. W. Boyd, "Breaking lorentz reciprocity to overcome the time-bandwidth limit in physics and engineering," Science **356**(6344), 1260-1264 (2017).
7. S. Raghu and F. D. M. Haldane, "Analogs of quantum-Hall-effect edge states in photonic crystals," Phys. Rev. A **78**(3), 033834 (2008).
8. Z. Wang, Y. D. Chong, J. D. Joannopoulos and M. Soljačić, "Reflection-free one-way edge modes in a gyromagnetic photonic crystal," Phys. Rev. Lett. **100**(1), 013905 (2008).
9. X. Ao, Z. Lin, and C. T. Chan, "One-way edge mode in a magneto-optical honeycomb photonic crystal," Phys. Rev. B **80**(3), 033105 (2009).
10. J. D. Joannopoulos, R. D. Meade, and J. N. Winn, *Photonic Crystals: Molding the Flow of Light*, 2 (Princeton University, 2008).

11. Z. Wang, Y. D. Chong, J. D. Joannopoulos, and M. Soljačić, "Observation of unidirectional backscattering-immune topological electromagnetic states," Nature **461**(7265), 772-775 (2009).
12. H. Raether, *Surface Plasmons* (Springer, 1988).
13. Z. Yu, G. Veronis, Z. Wang, and S. Fan, "One-way electromagnetic waveguide formed at the interface between a plasmonic metal under a static magnetic field and a photonic crystal," Phys. Rev. Lett. **100**(2), 023902 (2008).
14. B. Hu, Q. J. Wang, and Y. Zhang, "Broadly tunable one-way terahertz plasmonic waveguide based on nonreciprocal surface magneto plasmons," Opt. Lett. **37**(11), 1895-1897 (2012).
15. L. Shen, Y. You, Z. Wang, and X. Deng, "Backscattering-immune one-way surface magnetoplasmons at terahertz frequencies," Opt. Express **23**(2), 950-962 (2015).
16. X. Deng, L. Hong, X. Zheng, and L. Shen, "One-way regular electromagnetic mode immune to backscattering," Appl. Opt. **54**(14), 4608-4612 (2015).
17. J. J. Brion, R. F. Wallis, A. Hartstein, and E. Burstein, "Theory of surface magnetoplasmons in semiconductors," Phys. Rev. Lett. **28**(22), 1455-1458 (1972).
18. R. F. Wallis, J. J. Brion, E. Burstein, and A. Hartstein, "Theory of surface polaritons in anisotropic dielectric media with application to surface magnetoplasmons in semiconductors," Phys. Rev. B **9**(8), 3424-3437 (1974).
19. L. Shen, J. Xu, Y. You, K. Yuan, and X. Deng, "One-way electromagnetic mode guided by the mechanism of total internal reflection," IEEE Photonics Technol. Lett. **30**(2), 133-136 (2018).
20. B. Corcoran, C. Monat, C. Grillet, D. J. Moss, B. J. Eggleton, T. P. White, L. O'Faolain, and T. F. Krauss, "Green light emission in silicon through slow-light enhanced third harmonic generation in photonic-crystal waveguides," Nat. Photonics **3**, 206-210 (2009).
21. M. I. Stockman, "Nanofocusing of Optical Energy in Tapered Plasmonic Waveguides," Phys. Rev. Lett. **93**, 137404 (2004).
22. Y. A. Vlasov, M. O'Boyle, H. F. Hamann, and S. J. McNab, "Active control of slow light on a chip with photonic crystal waveguides," Nature **438**, 65-69 (2005).
23. K. L. Tsakmakidis, A. D. Boardman, and O. Hess, "Trapped rainbow storage of light in metamaterials," Nature **450**(7168), 397-401 (2007).
24. K. Liu, and S. He, "Truly trapped rainbow by utilizing nonreciprocal waveguides," Sci. Rep. **6**, 30206 (2016).
25. A. W. Snyder, and J. D. Love, *Optical Waveguide Theory* (Chapman and Hall, 1983).
26. T. H. Isaac, W. L. Barnes, and E. Hendry, "Determining the terahertz optical properties of subwavelength films using semiconductor surface plasmons," Appl. Phys. Lett. **93**(24), 241115 (2008).